HYDROTHERMAL SYNTHESIS OF KAOLINITE
AND ITS FORMATION MECHANISM

KYOUNG-WON RYU, YOUNG-NAM JANG*, AND SOO-CHUN CHAE

Korea Institute of Geoscience and Mineral Resources, Geological and Environmental Research Department, Daejeon 305-350, Korea

Abstract—In spite of many studies of kaolinite synthesis, questions remain as to the transformation of gel into kaolinite, the kinetics of the reaction, and the influence of solution chemistry. The purpose of the present study was to perform a hydrothermal synthesis in order to understand better the transformation from boehmite to kaolinite. Kaolinite was synthesized from amorphous SiO_2 and $Al(OH)_3 \cdot xH_2O$ at fixed temperature (250ºC) and pressure (30 bar). The initial pH of the solution was 2. The reaction time for the synthesis was varied from 2 to 36 h. The physical properties of synthesized kaolinite were characterized by X-ray diffraction (XRD), infrared spectroscopy (IR), nuclear magnetic resonance (NMR) spectroscopy, field-emission-scanning electron microscopy (FE-SEM), transmission electron microscopy (TEM), and energy dispersive spectrometry (EDS).

The early stage of kaolinite synthesis followed activation of amorphous $Al(OH)_3 \cdot xH_2O$ to initiate the reactions, *i.e.* ionization and subsequent crystallization of boehmite. The boehmite reacted continuously with Si^{4+} dissolved in solution and gradually transformed to disordered, lath-shaped boehmite. In XRD and IR patterns, the typical peaks of boehmite were weakened or disappeared following the reaction.

Structural transformation from boehmite to kaolinite occurred when the Al/Si ratio of the aluminosilicate was 1.0. The kaolinite formed was in the form of curved flakes and its crystallinity increased with reaction time. In the final stage of reaction the morphology of kaolinite changed from flaky to polygonal. The hexagonal, platy kaolinite was therefore developed to allow the gradual variation of the chemical composition, crystal structure, and morphology.

Key Words—Boehmite, Hexagonal, Kaolinite, Synthesis, Transformation.

INTRODUCTION

Many studies have been carried out on the synthesis of kaolinite and its formation mechanism during hydrothermal reaction (*e.g.* Nagy, 1995; Huertas *et al.*, 1999). Kaolinite has been synthesized by hydrothermal methods from amorphous gel, minerals, chemicals, *etc.* at temperatures >200ºC. Several studies have reported the effects of temperature and duration of synthesis on the rate of formation of the kaolinite (*e.g.* Huertas *et al*, 1993; Rayner, 1962), the morphology of the synthesized kaolinite (Tomura *et al.*, 1985; Fiore *et al.*, 1995; Huertas *et al.*, 2004), and the role of pH in the synthesis of kaolinite (La Iglesia and Martin-Vivaldi, 1972; Eberl and Hower, 1975; Satokawa *et al.*, 1994, 1996; Ryu *et al.*, 2008).

The mechanism of kaolinite formation suggests that platy kaolinite can be crystallized either on the basis of the sheet structure of the boehmite during an intermediate degree of supersaturation (Tomura *et al.*, 1985) or produced by metastable phase transformation (Small *et al.*, 1992; Small, 1993). The hexagonal crystals can otherwise be precipitated in solution by the influence of temperature and the composition of the starting material. Lath-shaped or elongated crystals have been reported to form at temperatures of <200ºC and at a Si/Al ratio of 1.0, whereas, platy crystals are favored at temperatures >200ºC in Si or Al-rich gels (Fiore *et al.*, 1995).

The chemical composition of the solution is one of the most important factors in the crystal-growth mechanism because of the necessity to stabilize Al in octahedral coordination and to allow the formation of $Si-O-^{VI}Al$ bonds. This has been achieved by decreasing the pH to the acid range or by using Al-complexing agents (Stiffert and Wey, 1972; La Iglesia and Martin-Vivaldi, 1975; La Iglesia *et al.*, 1976). Although these studies have contributed to a better understanding of the formation mechanism of kaolinite, questions still remain. The key points in terms of kaolinite formation are the mechanism of transformation of gel into kaolinite, the kinetics of the reaction, and the influence of solution chemistry (Fialips *et al.*, 2000; Satokawa *et al.*, 1994; Huertas *et al.*, 1999).

The application of a hydrothermal process to understand the transformation mechanism from boehmite to kaolinite at different reaction times is described here.

EXPERIMENTAL METHODS

The experiment was conducted in a 1 L cold-seal-type stainless steel autoclave in which the solution and

* E-mail address of corresponding author:
crystal@kigam.re.kr

reacting materials were agitated continuously at 180 rpm. The starting materials for the synthesis of kaolinite were silica gel (Merck, Germany) and amorphous $Al(OH)_3 \cdot xH_2O$ (Aldrich, ~50−55% Al_2O_3). The molar ratio of the Al/Si of the starting material was 1.0 and the pH of the solution was controlled by adding 5% HCl solution (Dongyang Chem., extra pure) before the experiment. The initial pH of the solution was 2 and the final pH was always ~2.5−2.6. The following experimental conditions were maintained unless otherwise specified: chemical composition, $Al_2O_3/SiO_2 = 0.5$; temperature, 250ºC; pressure, 40 bar; and pH, 2.0. The reaction time was varied from 2 to 36 h.

The product was prepared as randomly oriented clay-aggregate specimens and analyzed by XRD (X'pert MPD Phillips Co) using CuKα radiation in conjunction with a diffracted beam graphite monochromator. The cation structure information was studied by ^{29}Si and ^{27}Al NMR spectroscopy (DSX 400MHz, Bruker Analyticsche GmbH) operated at 79.5 MHz for ^{29}Si and 104.3 MHz for ^{27}Al. Powdered samples were packed into rotors and spun in a magic-angle spinning probe at ~10 kHz and 14 kHz for Si and Al, respectively.

Fouier-transform infrared spectra (FTIR, Nicolet 380, Thermo Electron Corporation) were determined in the frequency range 400−4000 cm^{-1} with a resolution of 4 cm^{-1}. The spectra were obtained through transmission mode by KBr pressed pellets, which were prepared by homogeneous mixing of 1 mg of sample with 150 mg of KBr.

Morphological observations of the synthesized products were conducted by TEM (JEM2200FS, JEOL) coupled with an EDS (Oxford) and by scanning electron microscopy (FE-SEM, S-4700, Hitachi). The TEM instrument was operated at 200 kV. The samples were dispersed in distilled water by an ultrasonic probe, then placed on the holder and air-dried. Examination by SEM was carried out at a working voltage of 10 keV. For SEM study, the sample powder was sedimented onto Cu-micro grids and coated with osmium tetroxide (OsO_4).

RESULTS

X-ray diffraction patterns (Figure 1) illustrate the change in phases during synthesis of kaolinite at different reaction times. After 2 h of reaction, the starting material, i.e. amorphous $Al(OH)_3$, transformed to boehmite (AlOOH), but the silica gel remained unreacted throughout. After a reaction time of 5 h, the 020 and 120 peaks of boehmite were absent, thereby indicating that the crystal structure had been partially destroyed.

The formation of kaolinite was identified in the product obtained after 10 h of reaction. The 001, 002, and 060 reflections were very weak and the (02, 11) and (13, 20) diffraction bands were observed as nearly

unresolved with broad peaks. After 15 h of reaction time, the peak intensity of the 001 reflection showed approximately the same intensity as that of the (02, 11) band and the 002 peak. Non-basal diffraction bands of kaolinite (02, 11) and (13, 20) were sharp, asymmetrical, and either poorly resolved or rarely resolved. After 36 h of reaction time, kaolinite was formed with good crystallinity and the 001 reflection was found at 7.24 Å.

The angular breadth and symmetry of the basal reflections and the lattice spacing were also characteristic of kaolinite. For well ordered kaolinite, this reflection was sharp and symmetrical and the lattice spacing was in the range ~7.15−7.17 Å (Brindley et al., 1963). Therefore, the results of XRD indicated that the synthetic kaolinite was poorly ordered.

The MAS/NMR spectra of ^{29}Si and ^{27}Al from the synthetic kaolinite were compared to those from natural kaolinite from Georgia (Figure 2). A sharp single-line ^{27}Al spectrum was observed at 1.59 ppm for the synthetic phase, a value that is within the typical range of 0−10 ppm for 6-coordinated Al with O (Kirkpatrick and Phillips, 1993). In Georgia kaolinite this band was observed as a single line at 1.08 ppm (Figure 2). The ^{29}Si chemical shift in the NMR spectrum for the synthetic kaolinite was at −91.35 ppm, which is almost identical to that of the Georgia kaolinite standard (−91.36 ppm) and is typical of Q_3 systems in which the Si atom is surrounded by three siloxy Si−O−Si bridging groups (Slade and Davies, 1989).

The FTIR spectra were important in understanding the formation mechanism of kaolinite (Figure 3). After 2 h of reaction time, the peaks at 3091 and 3317 cm^{-1} corresponded to an Al−OH vibration and peaks at 408, 476, 626, and 742 cm^{-1} related to AlO_6 vibrations were observed. The Al−O stretching vibration at 742 cm^{-1} and the Al−O bending vibration at 408 cm^{-1} are characteristic features of boehmite with 6-fold coordinated Al. A typical spectrum of boehmite contains two
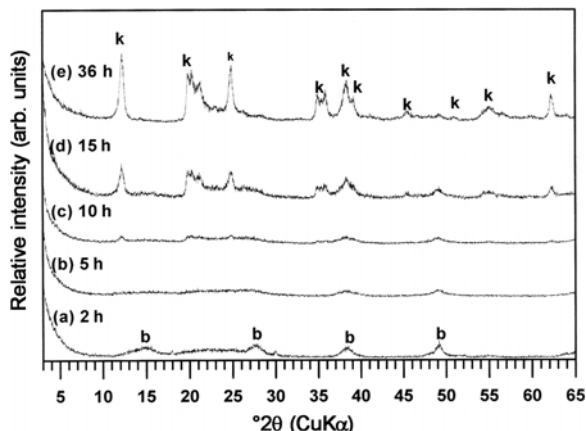

Figure 1. XRD patterns of synthetic kaolinite for each of five reaction times: (a) 2 h, (b) 5 h, (c) 10 h, (d) 15 h, and (e) 36 h.
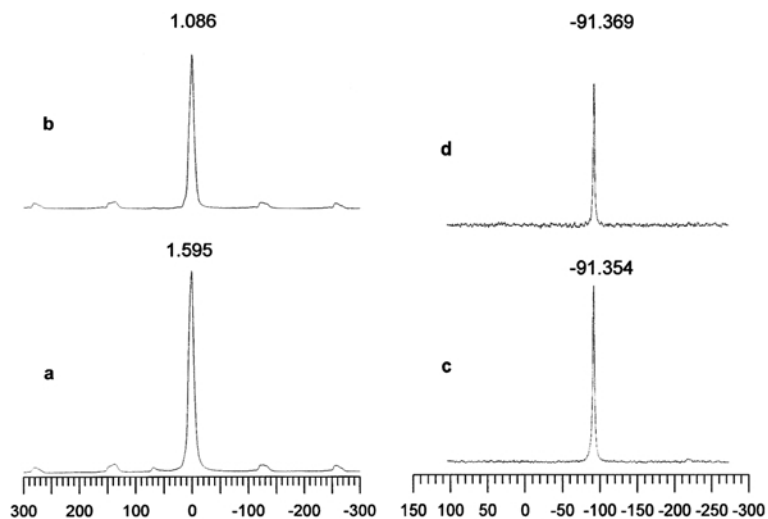
Figure 2. ^{27}Al MAS NMR spectra of synthetic kaolinite (a) and Georgia kaolinite (b), and ^{29}Si MAS NMR spectra of synthetic kaolinite (c), and Georgia kaolinite (d).
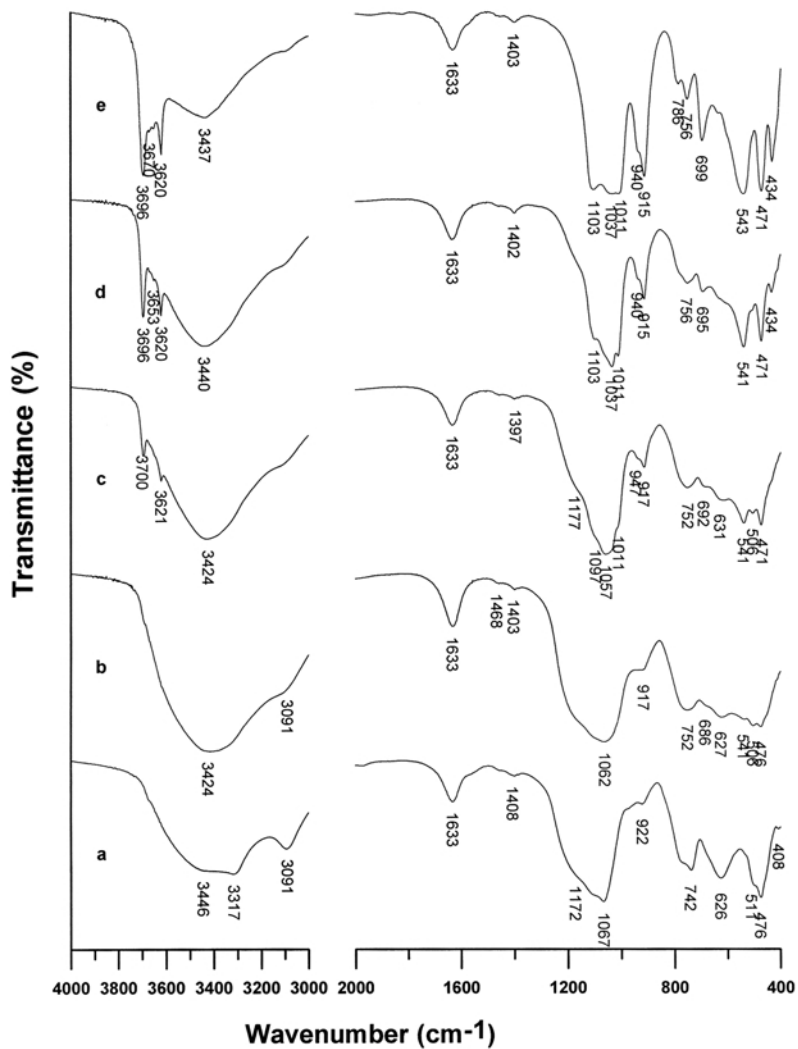

Figure 3. IR spectra of synthesized kaolinite for each of five reaction times: (a) 2 h, (b) 5 h, (c) 10 h, (d) 15 h, and (e) 36 h.

strong and well separated Al−OH absorption bands at 1157 cm^{-1} and 1068 cm^{-1}. This study revealed only a single broad, strong peak at 1067 cm^{-1}, which clearly indicates the formation of an O−Si−O−Al−OH vibration from the reaction of Si−O and Al−OH. The incorporation of Si in the boehmite structure thus initiated the transformation process of boehmite into kaolinite (Figure 3a).

After 5 h of reaction, the Al−OH stretching band at the largest wavenumber of 3424 cm^{-1} was a very strong and broad band with a shoulder at 3091 cm^{-1}. The Al−OH bending vibration at 1067 cm^{-1} shifted to lower frequency and became somewhat broader. The characteristic peak of boehmite at 742 cm^{-1} shifted to a slightly larger wavenumber (752 cm^{-1}) and became broader and weaker. A newly formed peak at 541 cm^{-1} was also observed. The latter two peaks corresponded to Si−O−Al^{VI} compounded vibrations and are attributed to a continuous reaction between boehmite and Si. The Al−O bending vibration at 408 cm^{-1} disappeared at the same time (Figure 3b). The significant reduction of the peak intensity of boehmite clearly indicated the transformation of boehmite to kaolinite during this period. Similar results were also obtained during the XRD study (Figure 1b).

After 10 h of reaction, Al$_2$O−H stretching bands of kaolinite at 3700 cm^{-1} and 3621 cm^{-1} were observed, but no peaks at 3670 cm^{-1} and 3653 cm^{-1} in between were seen. The band at 1057 cm^{-1}, assigned to the Si−O−Si symmetric stretching vibration, became stronger. The band at 1097 cm^{-1} assigned to Si−O stretching hydrogen bonded to H$_2$O, and the 1011 cm^{-1} band assigned to Si−O−Si symmetric stretching vibration, showed weak shoulders. Another characteristic, new band of kaolinite, located at 947 cm^{-1}, was assigned to Al$_2$O−H which may be due to the deformation of internal free OH. On the other hand, the intensity of the band at 917 cm^{-1} assigned to Al$_2$O−H, which occurred due to the deformation of internal-surface OH, increased with reaction time but the intensity was weak. Sharp bands of moderate intensity were observed at 541 cm^{-1} and 471 cm^{-1} for Si−O−Al^{VI} and Si−O−Si deformation bending vibrations, respectively, which increased with increasing reaction time (Figure 3c).

As discussed above, the increase in intensity of the bands and appearance of new peaks are attributed to the beginning of the crystallization of a poorly ordered kaolinite and the disappearance of boehmite, endorsing the results obtained from the XRD study.

As per the IR patterns, a well ordered kaolinite was successfully obtained when the reaction time was increased to 15 h. The four characteristic hydroxyl bands of kaolinite were well resolved although the bands at 3670 and 3653 cm^{-1} were poorly developed. The development of the hydroxyl stretching bands between 3700 and 3620 cm^{-1} depends on the degree of order and crystalline perfection (Farmer, 1974; van der Marel and

Beutelspacher, 1976; Rusell, 1987; Zhang and Xu, 2007).

The Si−O stretching region comprised three absorption bands at 1103, 1037, and 1011 cm^{-1}, which were well resolved. The intensity of the doublet at 940 and 915 cm^{-1} assigned to the Al$_2$O−H vibration and the bands at 541 and 474 cm^{-1} assigned to the Si−O−Al vibration became stronger. A new kaolinite peak at 434 cm^{-1} appeared. The bands for gibbsite-like layers of kaolinite were shifted to larger wavenumbers, 756 and 695 cm^{-1}. The band at 786 cm^{-1} was observed as a weak shoulder (Figure 3d).

The IR analysis above revealed that the crystallinity of synthetic kaolinite improved and a structurally well ordered kaolinite appeared when the reaction time was increased to 15 h. The XRD study suggested that kaolinite was fully developed at the expense of boehmite at this stage of reaction.

A highly ordered kaolinite was obtained after 36 h of reaction. At small wavenumbers, the spectrum showed the in-plane Si−O vibrations at 1103, 1037, and 1011 cm^{-1}, comprising both well ordered and poorly ordered kaolinite. The Al−OH band at 940 cm^{-1}, assigned to the inner OH-surface, occurred as a small inflection on the OH-bending vibrations and inner-hydroxyl groups at 915 cm^{-1} were apparently sharp during the transition. These two peaks particularly represented characteristic absorption modes of kaolinite. Sharp stretching bands for Si−O at 699 cm^{-1} and the Si−O−Al compounded vibration at 786 and 756 cm^{-1} were observed. The bands at 543, 471, and 434 cm^{-1}, assigned to the in-plane Al−O−Si and Si−O−Si bending vibrations, were also sharp and represent a well ordered kaolinite.

The surface morphology of the synthesized kaolinite was analyzed using SEM and TEM (Figures 4, 5). Boehmite particles were 50−100 nm in diameter with partially rounded outline or lath-type morphology after 2 h of reaction (Figures 4a, 5a). The morphology remained virtually unchanged until 5 h of reaction (Figure 5b), but the crystal size decreased (Figure 4b). This was interpreted as a partial dissolution of boehmite related to the incorporation of Si into the structure. The results corresponded with those from the XRD and IR studies.

After 10 h of reaction time, the shape of the particles changed from rounded or lath-shaped to curved flakes with a noticeable increase in particle size. The particle surface was smooth and curved, but the outlines were rarely polygonal. Curled or tubular forms and some platy forms indicated the high degree of disorder with respect to both the 'a' and 'b' axes (Brindley et al., 1963). A number of round, lath-shaped crystals, regarded as aluminosilicates, remained unreacted in the reaction (Figure 4c). The electron diffraction pattern was typical of well crystallized kaolinite and showed the presence of pseudo-hexagonal structure (Figure 5c).
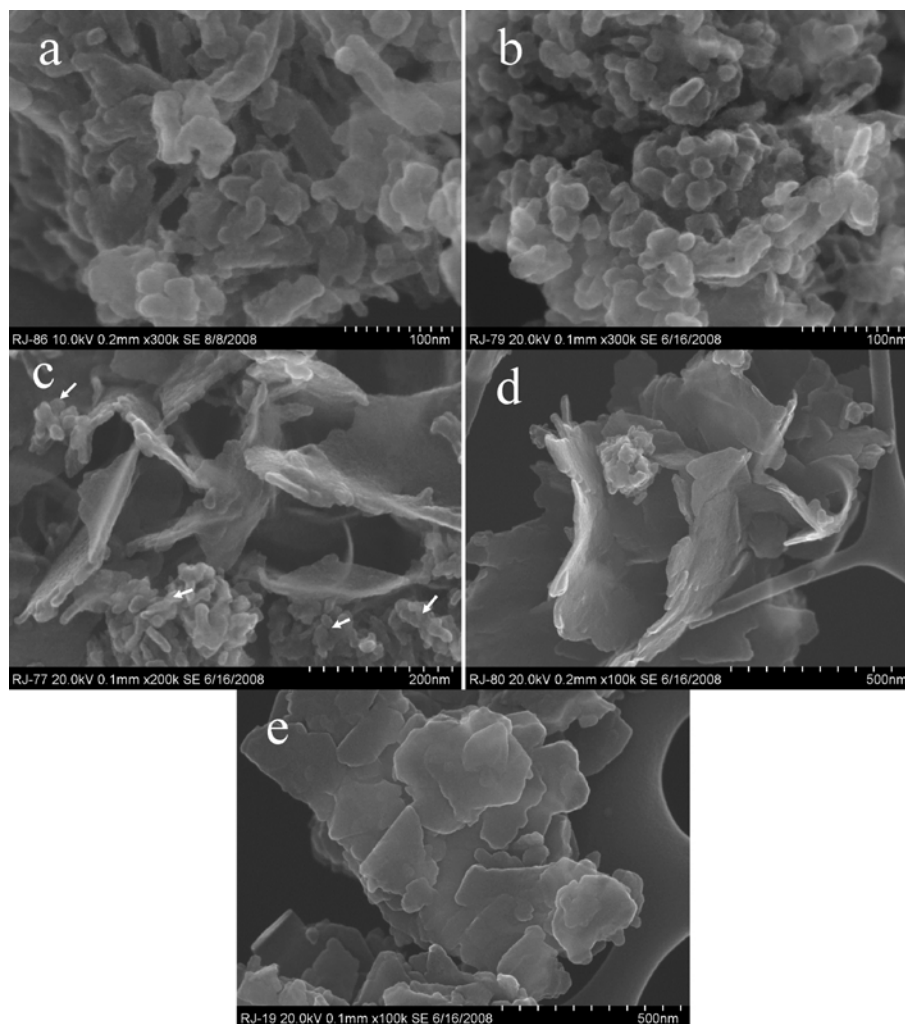
Figure 4. SEM images of synthesized kaolinite after each of five reaction times: (a) 2 h, (b) 5 h, (c) 10 h, (d) 15 h, and (e) 36 h. Arrows in (c) indicate grains of aluminosilicates.

After 15 h of reaction, almost all of the lath-type shape had disappeared and the curved platy phase dominated the SEM images. The particle shape was similar to that of the '10-h product,' but the particle size had increased. Kaolinite may have shown a greater degree of order (Figure 4d). The (001) plane was wider and thin leaves of variable shape were observed by TEM (Figure 5d).

After 36 h, the morphology of synthetic kaolinite exhibited platy crystals with partial polygonal outlines. Its pseudo-hexagonal symmetry was identified in the electron diffraction patterns with the beam direction parallel to (001), indicating that increasing reaction time was a critical factor in the formation of the well crystallized kaolinite (Figures 4e, 5e).

The EDS analysis showed a range of Al/Si ratios from 2.4 to 1 (Figure 6). A considerable amount of Si was found in the lath-shaped boehmite after 2 h of

reaction. The detection of Si indicated the reaction of boehmite and silica. These observations were in good accord with those made using IR and XRD. The rounded crystals were identified as amorphous silica. After 15 h of reaction time, the flaky shaped kaolinite revealed an Al/Si ratio of 1.0.

DISCUSSION

In the Al_2O_3-H_2O system, the thermodynamic stability showed amorphous $Al(OH)_3$ < gibbsite < boehmite < diaspore in the temperature range of ~200−300ºC (Kittrick, 1966). Amorphous aluminum hydroxide ($AlOH_3$) can be transformed easily to boehmite although differences arise according to the reaction temperature, pH, and solution chemistry (Robins, 1967). Moreover, at room temperature, Al solubility is greater than that of Si in an acidic medium. Mason (1966) showed that low pH
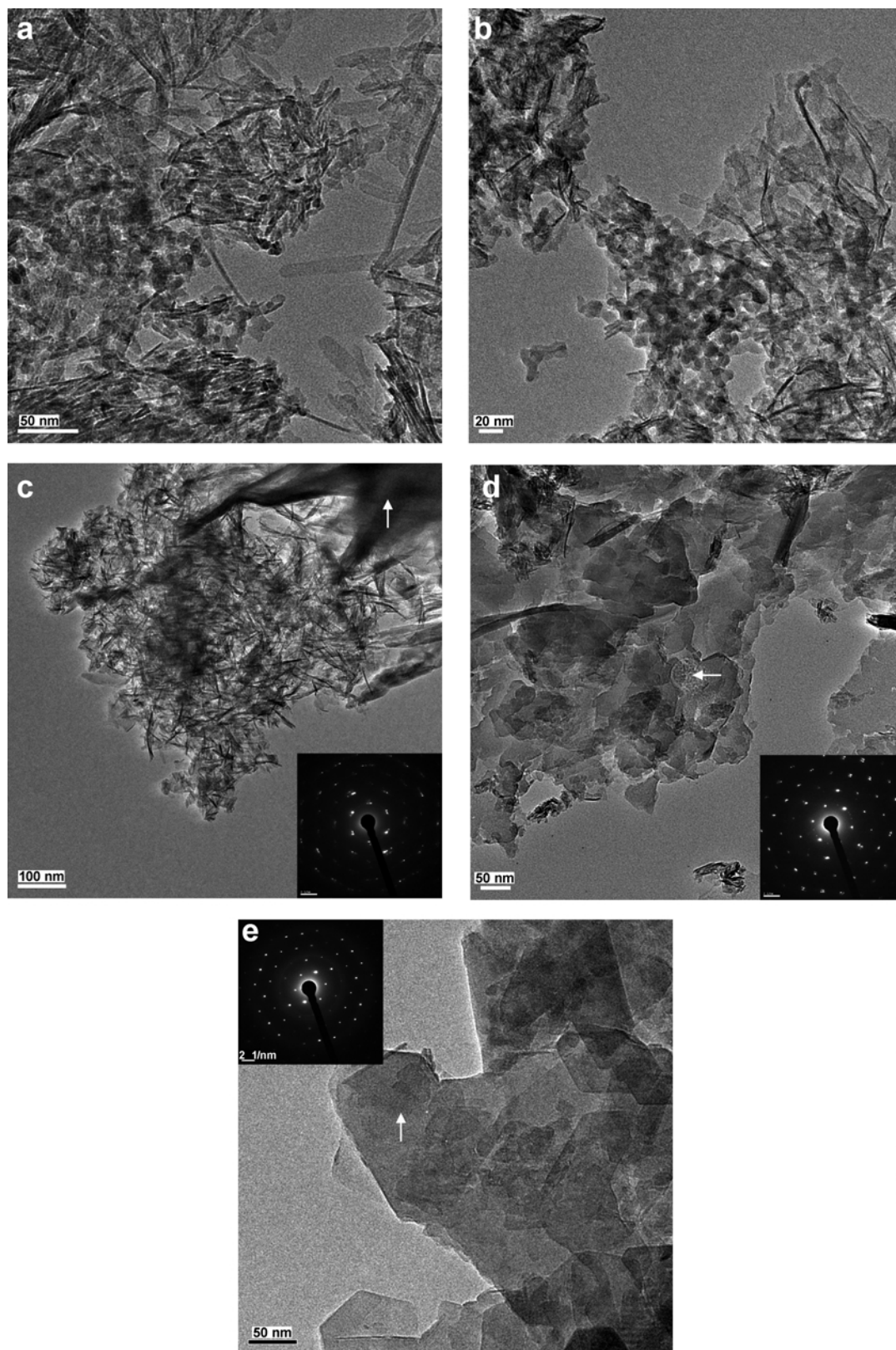
Figure 5. TEM images of synthesized kaolinite after each of five reaction times: (a) 2 h, (b) 5 h, (c) 10 h, (d) 15 h, and (e) 36 h. Arrows indicate the points for SAED.

favors the formation of 6-coordinated Al and dominant kaolinite crystallization. Satokawa *et al.* (1996) carried out an experiment at 220ºC and pH 2.7 and proposed that the kaolinite with platy morphology should crystallize on the basis of the sheet structure of boehmite.

Boehmite crystallization was observed clearly by means of XRD and IR in the product that reacted for 2 h. The reaction of boehmite with silica was identified by the appearance of an IR peak at 1067 cm^{-1} which was not typically pure boehmite, indicating the incorporation of Si in the boehmite structure. In addition, some Si (atomic ratio of Al:Si = 2.4:1 on average) in boehmite was detected by EDS (Figure 6).

With prolonged autoclaving for 5 h, however, boehmite was transformed to a transitional phase which is characterized by the disappearance of several IR and XRD peaks of boehmite. The corresponding SEM and TEM observations of the samples showed that the morphology was not changed but the particle size had decreased, suggesting the partially soluble nature of boehmite. Other clues for the transformation were the appearance of new peaks or a variation of the typical IR pattern of boehmite, a somewhat displaced Si−O−Al^{VI} bond, and gibbsite-like layers of kaolinite due to the dissolution of boehmite and the addition of Si from silica, the IR bands of which are completely different from the AlO$_6$ bands of pure boehmite.

After a reaction time of 10 h, poorly crystallized kaolinite formed with some boehmite in the product itself. Almost all of the crystals were in the shape of curved flakes and the EDS spectra showed the major constituents to be Al and Si, approaching the stoichiometric composition of kaolinite. Furthermore, as the reaction time increased (15 h), the IR and XRD analyses

displayed the characteristic kaolinite patterns with highly improved crystallinity as boehmite disappeared eventually. At the same time the synthetic kaolinite showed a partially rounded and irregular platy form.

After 36 h of reaction time, the morphology exhibited nearly individual polygonal plates with pseudo-hexagonal symmetry in the electron diffraction pattern. The chemical composition of kaolinite after ~15−36 h of reaction was very similar to that after 10 h, suggesting that 10 h of reaction time would be sufficient to complete the kaolinite-formation reaction. The next step would be the gradual transformation of the structure and its simultaneous change in shape from lath-shaped to flakey.

Boehmite contains double sheets of octahedra with ions at the center, and the sheets themselves are composed of chains of octahedra, while kaolinite also has octahedral coordination with a layered structure. The double sheets of boehmite would become disordered due to the continuous adsorption of Si into the structure, resulting in the rearrangement of the structure and the transformation of the 1:1 layered structure. The destruction of boehmite and the formation of kaolinite are closely related to each other, as indicated in the results of the IR study. The boehmite structure was stable until the chemical composition of the aluminosilicate reached Al/Si<1. This strongly suggests that the formation mechanism of kaolinite is the transformation based on the boehmite, rather than precipitation from solution.

After the XRD and IR results, kaolinite eventually became a stable phase and its crystallinity increased with increasing reaction time. When the 'structural perfection' was accomplished, its morphology changed from flaky to hexagonal plates in accordance with the reaction time.

Microscopy, X-ray diffraction, and infrared spectra observations suggested that the activation of Al(OH)$_3$·xH$_2$O should be required to initiate the transformation reaction, *i.e.* ionization and subsequent crystallization of boehmite in the early stage of the kaolinization. Thereafter, the continuous reaction between boehmite and the Si^{4+} in solution resulted in the formation of kaolinite. The hexagonal platy kaolinite was, therefore, grown on the basis of boehmite according to gradual variation of the chemical composition, crystal structure, and surface morphology.

CONCLUSIONS

The transformation mechanism of boehmite into kaolinite during the hydrothermal synthesis was investigated systematically. The kaolinization process in acidic conditions consisted of three consecutive stages.

During the first stage, the ionization of amorphous Al(OH)$_3$·xH$_2$O and subsequent crystallization of boehmite occurred. Al(OH)$_3$ was initially transformed to boehmite over a 2 h period, as the acidic environment
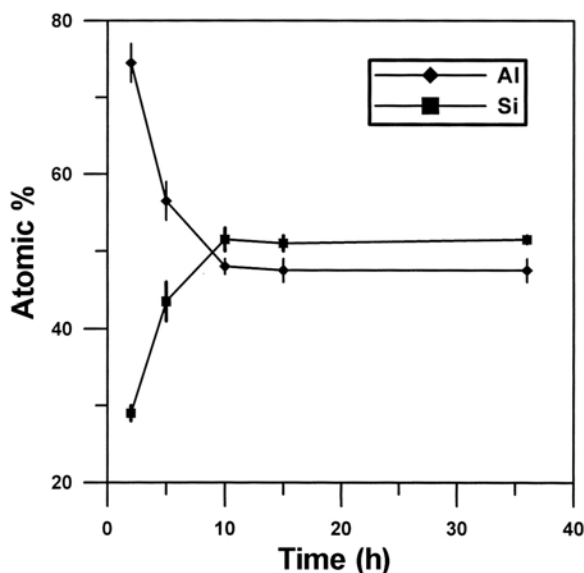

Figure 6. EDS data for Al and Si of the synthesized kaolinite.

appeared to favor the formation of boehmite. Boehmite then adsorbed Si^{4+} continuously and gradually transformed to disordered boehmite. The boehmite structure was unchanged until the chemical composition of the disordered boehmite was Al/Si<1.0. The disordered boehmite had a lath-type morphology.

The boehmite and kaolinite coexisted during the second stage. The chemical composition of the aluminosilicate approached the stoichiometry Al/Si = 1.0 along with the structural transformation to kaolinite. The kaolinite became stable after 10 h of reaction time while its crystallinity increased with increasing reaction time and it became flaky in shape. During the final stage, the morphology of kaolinite changed from flaky to polygonal.

ACKNOWLEDGMENTS

REFERENCES

Brindly, G.W., Santos, P.S., and Santos, H.S. (1963) Mineralogical studies of kaolinite-halloysite clays: Part I, Identification problems. *American Mineralogist*, **48**, 897−910.

Eberl, D.D. and Hower, J. (1975) Kaolinite synthesis; the role of the SiAl and (alkali)/(H^+) ratio in hydrothermal systems. *Clays and Clay Minerals*, **23**, 301−309.

Farmer, V.C. (1974) *The Infrared Spectra of Minerals*. Monograph **4**, Mineralogical Society, London.

Fialips, C.I., Petit, S., Decarreau, A., and Beaufort, D. (2000) Influence of synthesis pH on kaolinite crystallinity and surface properties. *Clays and Clay Minerals*, **48**, 173−184.

Fiore, S., Huertas, F.J., Huertas, F., and Linares, J. (1995) Morphology of kaolinite crystals synthesized under hydrothermal conditions. *Clays and Clay Minerals*, **43**, 353−360.

Huertas, F.J., Huertas, F., and Linares, J. (1993) Hydrothermal synthesis of kaolinite: method and characterization of synthetic materials. *Applied Clay Science*, **7**, 345−356.

Huertas, F.J., Fiore, S., Huertas, F., and Linares, J. (1999) Experimental study of the hydrothermal formation of kaolinite. *Chemical Geology*, **156**, 171−190.

Huertas, F.J., Fiore, S., and Linares, J. (2004) In-situ transformation of amorphose gel into spherical aggregates of kaolinite: a TEM study. *Clay Minerals*, **39**, 423−431.

Kirkpatrick, R.J. and Phillips, B.L. (1993) ^{27}Al NMR spectroscopy of minerals and related materials. *Applied Magnetic Resonance*, **4**, 213−236.

Kittrick, J.A. (1966) The free energy of formation of gibbsite and $Al(OH)_4^-$ from solubility measurements. *Soil Science Society of America Proceedings*, **30**, 595−598.

La Iglesia, A. and Martin Vivaldi, J.L. (1972) A contribution to the synthesis of kaolinite. In: *Proceedings of the International Clay Conference, Madrid*, pp. 173−185.

La Iglesisa, A. and Martin-Vivaldi, J.L. (1975) Synthesis of kaolinite by homogeneous precipitation at room temperature: I. Use of anionic resin in (OH) form. *Clay Minerals*. **10**, 399−405.

La Iglesia, A., Martin-Vivaldi, J.L. and Lopez-Aguayo, F., Jr. (1976) Kaolinite crystallization at room temperature by homogeneous precipitation: III. Hydrolysis of feldspars. *Clays and Clay Minerals*, **24**, 36−42.

Mason, B. (1966) *Principles of Geochemistry*, 3rd edition. John Wiley and Sons, Inc., New York, pp. 164−167.

Nagy, K.L. (1995) Dissolution and precipitation kinetics of sheet silicates. Pp. 173−233 in: *Chemical Weathering Rates of Silicate Minerals* (A.F. White and S.L. Brantley, editors). Reviews in Mineralogy, **31**. Mineralogical Society of America, Washington, D.C.

Rayner, J.H. (1962) An examination of the rate of formation of kaolinite from a coprecipitated silica gel. In: *Colloque sur la Gènese et al Synthèse des Argilles*, C.N.R.S., No. 105. Paris, pp. 123−127.

Robins, R.G. (1967) Hydrothermal precipitation in solutions of thorium nitrate, ferric nitrate and aluminium nitrate. *Journal of Inorganic Nuclear Chemistry*, **29**, 431−435.

Rusell, J.D. (1987) Infrared methods. Pp. 133−172 in: *A Handbook of Determinative Methods in Clay Mineralogy* (M.J. Wilson, editor). Chapman & Hall, London.

Ryu, K.W., Jang, Y.N., Chae, S.C., Bae, I.K., and Lee, S.K. (2008) The characterization of kaolinite synthesized according to the pH. *Korea Society of Economic and Environmental Geology*, **41**, 165−172.

Satokawa, S., Osaki, Y., Samejima, S., Miyawaki, R., Tomura, S., Shibasaki, Y., and Sugahara, Y. (1994) Effects of the structure of silica-alumina gel on the hydrothermal synthesis of kaolinite. *Clays and Clay Minerals*, **42**, 288−297.

Satokawa, S., Miyawaki, R., Osaki, Y., Tomura, S., and Shibasaki, Y. (1996) Effects of acidity on the hydrothermal synthesis of kaolinite from silica-gel and gibbsite. *Clays and Clay Minerals*, **44**, 417−423.

Slade, R.C.T. and Davies, T.W. (1989) The mechanism of kaolinite dehydroxylation followed by high resolution ^{27}Al NMR and ^{29}Si NMR. *Colloids and Surfaces*, **36**, 119−125.

Small, J.S. (1993) Experimental determination of the rates of precipitation of authigenic illite and kaolinite in the presence of aqueous oxalate and comparison to the K/Ar ages of authigenic illite in reservoir sandstones. *Clays and Clay Minerals*, **41**, 191−208.

Small, J.S., Hamilton, D.L., and Habesch, S. (1992). Experimental simulation of clay precipitation within reservoir sandstones: 1. Techniques and examples. *Journal of Sedimentary Petrology*, **62**, 508−519.

Stiffert, B. and Wey, R. (1972) Contribution a la connaissance de lasynthese des kaolins. In: *Proceeding of International Clay Conference, Madrid*, pp. 159−172.

Tomura, S., Shibasaki, Y., Mizuta, H., and Kitamura, M. (1985) Growth conditions and genesis of spherical and platy kaolinite. *Clays and Clay Minerals*, **33**, 200−206.

Van der Marel, H.W. and Beutelspacher, H. (1976) *Atlas of Infrared Spectroscopy of Clay Minerals and their Admixtures*. Elsevier, Amsterdam.

Zhang, X.R. and Xu, Z. (2007) The effect of microwave on preparation of kaolinite/dimethylsulfoxide composite during intercalation process. *Materials Letters*, **61**, 1478−1482.